JB
Journals.ASM.org

Physiology and Bioenergetics of [NiFe]-Hydrogenase 2-Catalyzed H_2-Consuming and H_2-Producing Reactions in *Escherichia coli*

Constanze Pinske,[a] Monique Jaroschinsky,[b] Sabine Linek,[b] Ciarán L. Kelly,[a]* Frank Sargent,[a] R. Gary Sawers[b]

Division of Molecular Microbiology, University of Dundee, College of Life Sciences, Dundee, Scotland, United Kingdom[a]; Institute for Biology/Microbiology, Martin Luther University Halle-Wittenberg, Halle (Saale), Germany[b]

Escherichia coli **uptake hydrogenase 2 (Hyd-2) catalyzes the reversible oxidation of H_2 to protons and electrons. Hyd-2 synthesis is strongly upregulated during growth on glycerol or on glycerol-fumarate. Membrane-associated Hyd-2 is an unusual heterotetrameric [NiFe]-hydrogenase that lacks a typical cytochrome *b* membrane anchor subunit, which transfers electrons to the quinone pool. Instead, Hyd-2 has an additional electron transfer subunit, termed HybA, with four predicted iron-sulfur clusters. Here, we examined the physiological role of the HybA subunit. During respiratory growth with glycerol and fumarate, Hyd-2 used menaquinone/demethylmenaquinone (MQ/DMQ) to couple hydrogen oxidation to fumarate reduction. HybA was essential for electron transfer from Hyd-2 to MQ/DMQ. H_2 evolution catalyzed by Hyd-2 during fermentation of glycerol in the presence of Casamino Acids or in a fumarate reductase-negative strain growing with glycerol-fumarate was also shown to be dependent on both HybA and MQ/DMQ. The uncoupler carbonyl cyanide *m*-chlorophenylhydrazone (CCCP) inhibited Hyd-2-dependent H_2 evolution from glycerol, indicating the requirement for a proton gradient. In contrast, CCCP failed to inhibit H_2-coupled fumarate reduction. Although a Hyd-2 enzyme lacking HybA could not catalyze Hyd-2-dependent H_2 oxidation or H_2 evolution in whole cells, reversible H_2-dependent reduction of viologen dyes still occurred. Finally, hydrogen-dependent dye reduction by Hyd-2 was reversibly inhibited in extracts derived from cells grown in H_2 evolution mode. Our findings suggest that Hyd-2 switches between H_2-consuming and H_2-producing modes in response to the redox status of the quinone pool. Hyd-2-dependent H_2 evolution from glycerol requires reverse electron transport.**

In 1937, Krebs found that *Escherichia coli* cells are able to use hydrogen or glycerol to reduce fumarate, yielding succinate (1). Today, it is known that the enzymes [NiFe]-hydrogenase (Hyd), glycerol dehydrogenase, and fumarate reductase (FRD) are involved in this process. Under anaerobic conditions, *E. coli* is able to synthesize two uptake Hyd complexes, termed Hyd-1 and Hyd-2, that catalyze the oxidation of H_2 to protons and electrons (2, 3). Both enzymes face the periplasmic side of the cytoplasmic membrane and are translocated as a large- and small-subunit complex by the Tat (twin arginine transport) protein translocation machinery. The Tat signal peptide is located on the N terminus of the respective small subunit (4). The two complexes differ in their expression patterns, oxygen tolerance, and subunit composition when associated with the cytoplasmic membrane (5–7). The Hyd-2 complex has an unusual architecture because, in addition to the large- and small-subunit heterodimer of HybC-HybO, a further two subunits, HybA and HybB, are required to complete a heterotetrameric complex on the periplasmic side of the membrane (7, 8). The HybA protein is a Tat-dependent protein with four predicted iron-sulfur cluster-binding sites, while HybB is an integral membrane protein with no known cofactors (7). It is still unknown how the assembly of the heterotetramer is coordinated subsequent to transport and membrane integration of the component parts.

A third hydrogenase, Hyd-3, forms part of the cytoplasmically oriented hydrogen-evolving formate hydrogenlyase complex (FHL), which oxidizes internally produced formate to CO_2 with the aid of formate dehydrogenase H (FDH-H) and uses the electrons to reduce protons to H_2 (2, 3, 9).

All Hyd large subunits contain a bimetallic [NiFe] cofactor at the active site, which is inserted through the concerted action of general Hyp accessory proteins and a further set of hydrogenase-specific "maturases" (2, 3). Maturation of the large subunit is completed with the proteolytic cleavage of a peptide at its C terminus and its subsequent association with the small subunit. This occurs prior to membrane association (10).

With the identification of distinct Hyd enzymes, it became possible to analyze their respective protein content and activities after growth under different conditions (11, 12). Thus, growth in glycerol-fumarate medium (GF medium) resulted in an increased content of Hyd-2 enzyme compared to growth in glucose medium (Glc medium) (12, 13). In contrast, Hyd-1 is more prevalent after growth in Glc medium than after growth in GF medium. Both uptake Hyd enzymes link H_2 oxidation to the reduction of quinones in the respiratory chain (14). As a result, hydrogen gas can serve as an electron donor for fumarate reductase (FRD) (15), which reduces fumarate to succinate. The heterotetrameric en-

Received 5 October 2014 **Accepted** 28 October 2014

Accepted manuscript posted online 3 November 2014

Citation Pinske C, Jaroschinsky M, Linek S, Kelly CL, Sargent F, Sawers RG. 2015. Physiology and bioenergetics of [NiFe]-hydrogenase 2-catalyzed H_2-consuming and H_2-producing reactions in *Escherichia coli*. J Bacteriol 197:296–306. doi:10.1128/JB.02335-14.

Editor: P. de Boer

Address correspondence to Frank Sargent, f.sargent@dundee.ac.uk, or R. Gary Sawers, gary.sawers@mikrobiologie.uni-halle.de.

* Present address: Ciarán L. Kelly, University of Oxford, Department of Biochemistry, Oxford, United Kingdom.

Supplemental material for this article may be found at http://dx.doi.org/10.1128/JB.02335-14.

doi:10.1128/JB.02335-14

zyme consists of the FrdABCD proteins, with FrdA being the catalytic subunit that contains a flavin adenine dinucleotide (FAD) cofactor. Although the FRD crystal structure revealed two quinone binding sites on opposite sides of the membrane, quinone-mediated proton translocation is not assumed, due to the lack of connecting heme groups (16).

Glycerol can also serve as an electron donor during fumarate respiration (1). Glycerol can be metabolized in the presence of electron acceptors by an ATP-dependent glycerol kinase (encoded by *glpK*) and subsequently by two quinone-dependent glycerol-3-phosphate dehydrogenases (encoded by *glpD* and *glpABC*), yielding dihydroxyacetone phosphate, an intermediate of glycolysis (summarized in reference 17). In addition, anaerobic glycerol utilization in the absence of external electron acceptors was shown to be possible if certain requirements were met (18). The key enzyme for glycerol activation to dihydroxyacetone is the NAD^+-linked glycerol dehydrogenase encoded by *gldA* (19, 20). At the same time, FRD is not required for glycerol fermentation (21). Recent studies have also revealed that during glycerol fermentation in the presence of Casamino Acids, Hyd-2 can evolve hydrogen (22), suggesting that under certain conditions the enzyme can function bidirectionally. This is in agreement with the electrochemical analysis of purified Hyd-2 (23). Therefore, in this study we wished to determine the requirements of Hyd-2 to function in H_2 evolution during fermentative growth with glycerol and in H_2 oxidation during respiratory growth on glycerol and fumarate. Our studies revealed unforeseen control of Hyd-2 enzyme activity in response to the redox status of the menaquinone pool, highlighted the importance of the HybA subunit in both H_2 oxidation and proton reduction, and identified a role for the proton gradient in coupling glycerol fermentation with H_2 evolution.

MATERIALS AND METHODS

Strains and growth conditions. All strains used in this study are listed in Table 1. *E. coli* strains were routinely grown at 37°C on LB agar plates or with shaking in LB broth (24). Anaerobic growth was performed at 37°C as standing liquid cultures. For phenotypic characterization, the cells were grown for at least 16 h in M9 minimal medium containing 1× M9 salts, 2 mM $MgSO_4$, 0.1 mM $CaCl_2$, 0.2% (wt/vol) Casamino Acids, 3 μM thiamine hydrochloride, trace element solution SL-A (25), 0.4% glycerol, and 25 mM sodium fumarate (26). When required, the antibiotics ampicillin, kanamycin, chloramphenicol, and spectinomycin were added to final concentrations of 100 μg ml^{-1}, 50 μg ml^{-1}, 12 μg ml^{-1}, and 100 μg ml^{-1}, respectively.

Genetic manipulations and plasmid construction. Cloning of the 3,430-bp *frdABCD* operon, including its native 118-bp promoter region, was done using MC4100 genomic DNA as the template for Herculase II (Agilent, USA) and the oligonucleotides frdA_fw_BamHI (5′-GCGGGA TCCATCAGACTATACTGTTG-3′) and frdD_rw_HindIII (5′-GCGAA GCTTAGATTGTAACGACACCAATC-3′). The PCR product was first ligated blunt into pJET1.2 (Thermo Fisher Scientific), and then it was excised and cloned into pACYCDuet-1 using BamHI and HindIII restriction sites. Similarly, the *menA* gene was cloned into pACYCDuet-1, including its native promoter, using the oligonucleotides menA_fw_BamHI (5′-GCGGGATCCGACTCCGGTATTAAACGC-3′) and menA_rw_HindIII (5′-GCGAAGCTTATGCTGCCCACTGGCTTAG-3′). The *hybA* gene was cloned into pJET1.2, including an artificial ribosome binding site, using the oligonucleotides hybA_fw_BamHI (5′-GCGG GATCCAGGAGGATAACCGTGAACAGACGTAATT-3′) and hybA_rw_HindIII (5′-CGCAAGCTTTCATGACTCATGATCGTCTCC-3′). The authenticity of the cloned DNA sequences was verified.

Construction of strain CP1A3 was done by transducing the Keio Δ*hybA* allele into IC010 by $P1_{kc}$-mediated transduction (24, 27). Similarly, strain CP1034 was constructed by introducing the Δ*hyfB-R*::Spc^r allele (which has a deletion of *hyfB* through *hyfR*) into IC010 (28) and IC012 was constructed by introducing the Keio Δ*menA* allele into IC010.

TABLE 1 Strains and plasmids

Strain or plasmid	Genotype[a]	Reference
Strains		
BW25113	F⁻ Δ(*araD-araB*)*567* Δ*lacZ4787*(::*rrnB-3*) λ⁻ *rph-1* Δ(*rhaD-rhaB*)*568 hsdR514*	27
MC4100	F⁻ *araD139* Δ(*argF-lac*)*U169* λ⁻ *rpsL150 relA1 deoC1 flhD5301* Δ(*fruK-yeiR*)*725* (*fruA25*) *rbsR22* Δ(*fimB-fimE*)*632*(::IS*1*)	51
DHP-F2	MC4100 Δ*hypF*	42
FTD147	MC4100 Δ*hyaB hybC hycE*	52
FTD671	MC4100 Δ*hybA*	7
HDK200	MC4100 Δ*hybBC*	53
IC010	MC4100 Δ*hyaB hycE*	52
IC012	MC4100 Δ*hyaB hycE menA*::*kan*	This study
JW4115	BW25113 Δ*frdA*::*kan*	27
JW3901	BW25113 Δ*menA*::*kan*	27
JW5713	BW25113 Δ*ubiC*::*kan*	27
JW5581	BW25113 Δ*ubiE*::*kan*	27
JW0659	BW25113 Δ*ubiF*::*kan*	27
CP887	MC4100 Δ*frdA*::FRT	This study
CP1034	MC4100 Δ*hyaB hycE hyfB-R*::Spc^r	This study
CP1037	MC4100 Δ*hyaB*::*kan hycAI*::*cat*	This study
SAL1	MC4100 Δ*hyaB*::FRT *hycAI*::FRT *frdA*::FRT	This study
CP1A3	MC4100 Δ*hyaB hycE hybA*::*kan*	This study
Plasmids		
pACYCDuet-frdAD	pACYCDuet-1, *frdA* promoter, *frdABCD*⁺ Cm^r	This study
pmenA	pACYCDuet-1, *menA* promoter, *menA*⁺ Cm^r	This study
pJET-hybA	pJET1.2, RBS-*hybA*⁺ Ap^r	This study

[a] Abbreviations: FRT, FLP recombination target; RBS, ribosome binding site.

PAGE and immunoblotting. Aliquots of 25 μg of protein from crude extracts were separated by SDS-polyacrylamide gel electrophoresis (PAGE) in 10% (wt/vol) gels (29) and transferred to nitrocellulose membranes as described previously (30). Antibodies raised against the Hyd-2 subunits (1:20,000), HycG (1:5,000) (31), TatC (1:3,000), and FdhE (1:3,000) were used. Secondary goat anti-rabbit antibody conjugated with horseradish peroxidase (HRP) enzyme (Bio-Rad, USA) was used for visualization of signals with the Immobilon Western chemiluminescent HRP substrate (Millipore, USA). Membrane preparations of crude extracts were made as described previously (11).

Enzyme activity assays. Hydrogenase in-gel activity staining using benzyl viologen (BV) and 2,3,5-triphenyltetrazolium chloride was done as previously described (32). Determination of total hydrogenase enzyme activity as H_2-dependent reduction of BV was performed according to the method in reference 11, except that the buffer used was 50 mM MOPS (morpholinepropanesulfonic acid), pH 7.0. The wavelength used was 600 nm, and an E_M (molar extinction coefficient) value of 7,400 M^{-1} cm^{-1} was assumed for reduced BV. Measurement of FRD activity as fumarate-dependent oxidation of reduced BV was performed according to the method in reference 33 in 50 mM MOPS, pH 7.0, at a wavelength of 600 nm. One unit of activity corresponded to the reduction of 1 μmol of substrate per min. Protein concentration was determined by the method of Bradford (Bio-Rad, USA) (34).

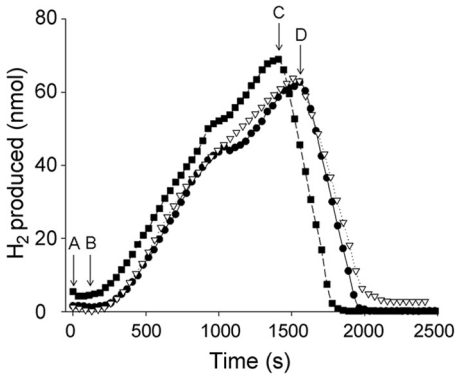

FIG 1 Hydrogenase 2 generates H_2 from glycerol and oxidizes H_2 using different electron acceptors. Cells for hydrogen production analysis on the hydrogen electrode were grown and prepared as described in Materials and Methods. Aliquots of 25 mg of cells from strain IC010 (Δ*hyaB hycE*), lacking Hyd-1 and Hyd-3 but synthesizing Hyd-2, were added at point A. After equilibration, glycerol was added to a final concentration of 170 mM at point B. After approximately 20 min, TMAO (squares, 67.5 mM final) was added at point C or fumarate (triangles, 25 mM final) or nitrate (circles, 60 mM final) was added at point D.

Cultures for measuring hydrogen production on the electrode were grown anaerobically for 16 h in LB plus 0.5% (vol/vol) glycerol and 34 mM fumarate. Cells were harvested and washed twice before resuspension in 1 ml per 1 g cells in 0.1 M sodium phosphate buffer, pH 6.8. Assays were carried out using a modified Clark-type electrode (Hansatech Oxygraph) calibrated with known amounts of H_2. The chamber was filled with 2 ml of buffer, and cells and substrates were added as indicated. In experiments in which methyl viologen (MV)-driven H_2 evolution was analyzed, cells were prepared as described above and MV was added to the chamber to a final concentration of 1.2 mM. Aliquots of a freshly prepared 10 mM sodium dithionite solution were added until the solution acquired a dark blue color, after which the evolution of hydrogen was monitored. As a negative control, the same procedure was performed, except that cells were omitted from the chamber. In experiments where carbonyl cyanide *m*-chlorophenylhydrazone (CCCP) was used, a 100 mM suspension in buffer was prepared to avoid using solvents that cells can use as electron acceptors, and it was added as a 1:1,000 dilution to the electrode chamber where indicated.

Gas chromatographic determination of hydrogen content in cultures was carried out in Hungate tubes filled with 5 ml of the respective medium, and the headspace was flushed with nitrogen. An aliquot of 200 μl gas phase from the headspace was analyzed on a Shimadzu GC-2010 Plus gas chromatograph. Pure nitrogen was used as the carrier gas, and the amount of produced hydrogen was calculated based on a standard curve.

RESULTS

Hyd-2 exhibits both proton-reducing and H_2-oxidizing activities. In order to demonstrate the bidirectionality of Hyd-2 *in vivo*, strain IC010 (Δ*hyaB hycE*), which lacks Hyd-1 and Hyd-3 (Table 1), was used. Harvested, washed intact cells were placed in the electrode chamber of an H_2-sensing electrode, and when exogenous glycerol was added, the cells initiated H_2 production (Fig. 1). The H_2 produced in the electrode chamber could be immediately reoxidized when external electron acceptors such as fumarate, trimethylamine *N*-oxide (TMAO), or nitrate were added to the chamber (Fig. 1). This indicates that Hyd-2 can rapidly switch between H_2 evolution and H_2 oxidation modes *in vivo*.

MQ and/or DMQ is required for electron transfer to and from Hyd-2 *in vivo*. As Hyd-2 couples hydrogen oxidation with fumarate reduction (12), we wanted to examine whether menaquinone (MQ) and demethylmenaquinone (DMQ) are involved in electron transfer to and from Hyd-2, the latter of which has been proposed (35) but never demonstrated (36). Therefore, strain IC012 was constructed by introducing a Δ*menA* mutation into strain IC010. Deletion of *menA* prevents synthesis of menaquinone and demethylmenaquinone but has no effect on ubiquinone biosynthesis (37). This strain grew very poorly anaerobically with glycerol and fumarate (GF), but sufficient cell material could be obtained to analyze the H_2-oxidizing activity of Hyd-2 using the viologen dye-linked in-gel hydrogenase activity staining procedure after nondenaturing, native PAGE (11). Surprisingly, the results of this analysis (Fig. 2A) revealed that no Hyd-2 activity could be detected in this strain after growth in GF medium; however, Hyd-2 activity was visible after fermentative growth with glucose (lane labeled Glc in Fig. 2A). Both the original isogenic parent strain IC010 and strain IC012 complemented with a plasmid carrying the *menA* gene revealed Hyd-2 activity after growth in GF medium.

Previous studies have shown that the H_2-oxidizing hydrogenases Hyd-1 and Hyd-2 have near-identical biochemical and physiological properties in *E. coli* wild-type strains MC4100 and BW25113 (38). Therefore, in order to test whether the deletion of *menA* caused the same Hyd-2 phenotype in the BW25113 background, we examined the activity of Hyd-2 in strain JW3901 (Δ*menA*). Indeed, no Hyd-2 activity after growth in GF medium could be observed, while Hyd-1 activity was unaffected (see Fig. S1 in the supplemental material).

Next, we examined Hyd-2 dye-reducing activity in strains lacking the genes encoding UbiC and UbiF, which are required for only ubiquinone (UQ) and not MQ/DMQ biosynthesis. After growth in GF medium, these strains exhibited both Hyd-1 and Hyd-2 enzyme activities like the wild type (see Fig. S1 in the supplemental material). As a further control, a mutation in *ubiE*, which prevents both UQ and MQ biosynthesis but allows DMQ synthesis (39), was analyzed. Extracts derived from the *ubiE* mutant retained a Hyd-1 and Hyd-2 enzyme activity pattern like that of the parent strain MC4100 (see Fig. S1). These results demonstrate that the H_2:benzyl viologen oxidoreductase activity of Hyd-2 is impaired in extracts of *menA* mutants but is unaffected in mutants lacking UQ.

It could be shown that the lack of measurable viologen dye-reducing activity of Hyd-2 was not due to a defect in Hyd-2 enzyme synthesis in the *menA* mutant, because when analyzed by Western blotting with anti-Hyd-2 antibodies, extracts derived from the strain showed nearly wild-type levels of the Hyd-2 large- and small-subunit antigens after growth in GF medium (see Fig. S2 in the supplemental material).

The effect of the *menA* mutation on H_2 production by Hyd-2 was examined in cells of strain IC012 (Δ*hyaB* Δ*hycE* Δ*menA*) (Fig. 2B). The cells of the isogenic parent strain IC010 produced H_2 at a rate of 1.7 nmol min^{-1} mg^{-1} when glycerol was used as the electron donor. In contrast, cells of IC012 failed to produce H_2 gas. This result indicates that MQ/DMQ mediates electron transfer for proton reduction catalyzed by Hyd-2. Examination of whole-cell H_2-oxidizing activity of strains IC010 and IC012 revealed that the *menA* mutant was unable to oxidize H_2 with fumarate as an electron acceptor (Fig. 2C). Finally, to demonstrate that the Hyd-2 enzyme was catalytically active in the *menA* mutant, IC012 was shown to be capable of catalyzing H_2 oxidation with nitrate as an

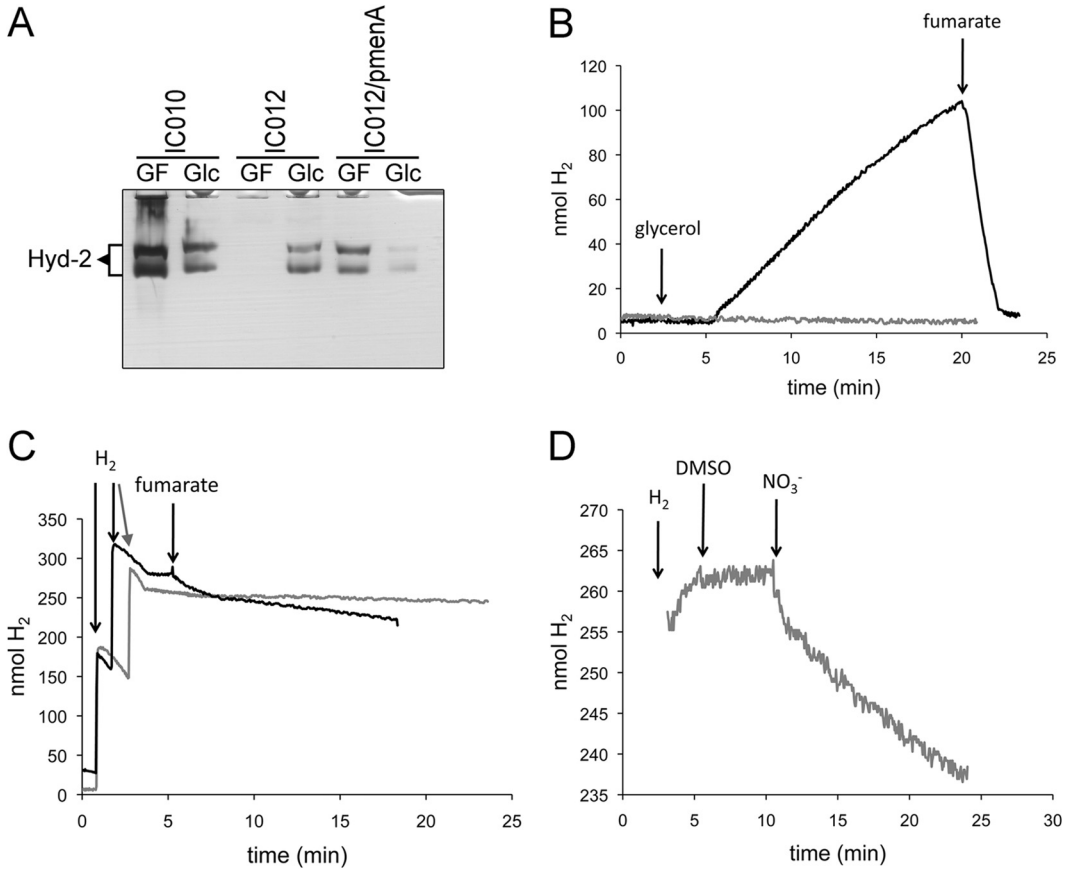

FIG 2 MQ/DMQ acts as a physiological electron donor and acceptor for Hyd-2. (A) Strains IC010 (Δ*hyaB hycE*) and IC012 (Δ*hyaB hycE menA*), as well as IC012 complemented with pmenA, were grown in GF medium (0.4% [wt/vol] glycerol and 25 mM fumarate) or Glc medium (0.8% [wt/vol] glucose), and extracts equivalent to 25 μg of protein were loaded on native PAGE gels and subsequently stained for hydrogenase activity as described in Materials and Methods. The migration position of Hyd-2 is labeled on the left side of the gel. (B) Strains IC010 (black line) and IC012 (gray line) were grown in GF medium, and cells corresponding to 5 mg of protein were analyzed for hydrogen production on the electrode. Glycerol was added to a final concentration of 170 mM and fumarate was added to a final concentration of 25 mM as indicated. (C) The same cells as in panel B (IC010, black; IC012, gray) were applied to the electrode, and H_2-saturated buffer was added as indicated before the addition of 25 mM fumarate. (D) H_2-saturated buffer was added to strain IC012 on the electrode, and DMSO (175 mM final concentration) and nitrate (60 mM final concentration) were subsequently added as indicated.

electron acceptor (Fig. 2D). This finding perhaps suggests that ubiquinone can couple Hyd-2-driven H_2 oxidation to nitrate reduction.

HybA is essential for reversible electron transfer between Hyd-2 and the quinone pool. The results of earlier studies strongly suggested that HybA is required for electron transfer from Hyd-2 to the quinone pool (7). To determine whether H_2 evolution by Hyd-2 also requires a functional HybA subunit, strain CP1A3 (Δ*hyaB hybA hycE*) was tested and proved to be unable to produce H_2 at a significant rate (Fig. 3A). Strain CP1034 (Δ*hyaB hycE hyfB-R*), which lacks Hyd-1 and Hyd-3, as well as the genes encoding Hyd-4 (28), was able to produce H_2 from glycerol at a rate of 4.14 nmol min^{-1} mg^{-1} when assayed on the H_2 electrode (Fig. 3A) and acted as a positive control for the experiment. This H_2-evolving activity of CP1034 was very similar to that determined for IC010 (Δ*hyaB hycE*) (Fig. 2B). H_2 production stopped abruptly upon addition of fumarate to the chamber, and the H_2 was rapidly and quantitatively oxidized. Together, these data show that the HybA subunit is required for Hyd-2 to mediate proton reduction.

To determine whether HybA is required to link H_2 oxidation by Hyd-2 to fumarate reduction, cells of CP1A3 were grown with glycerol and fumarate, washed, and incubated under 600 nmol H_2 and electron transfer to the quinone pool was examined after addition of fumarate (Fig. 3B). While strain CP1034 (Δ*hyaB hycE hyfB-R*) showed H_2-oxidizing activity, strain CP1A3 (Δ*hyaB hybA hycE*) lacking HybA failed to oxidize H_2. This demonstrates that HybA is also necessary for electron transfer from hydrogen to fumarate via menaquinone, as previously suggested (7).

HybA is not required for H_2:viologen dye oxidoreductase activity of Hyd-2. A strain with a deletion in the *hybA* gene retains active Hyd-2 enzyme in *in vitro* assays with viologen dyes (7, 40). Analysis of an extract derived from strain FTD671 (Δ*hybA*) by activity staining after native PAGE following growth in GF medium or in glycerol medium supplemented with Casamino Acids confirmed that Hyd-2 activity was detectable, but reduced, under both growth conditions (Fig. 4A). In contrast to extracts derived from MC4100 grown anaerobically with glycerol, Hyd-2 activity showed relief of inhibition of the H_2-dependent BV reductase activity in the Δ*hybA* strain FTD671 after growth under these conditions (compare Fig. 4A and 2A). Moreover, the pattern of the activity bands was different from that in MC4100, showing only

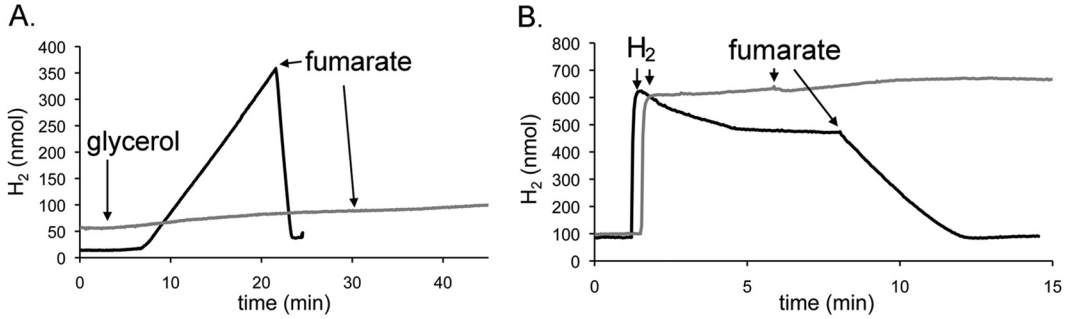

FIG 3 Role of the HybA subunit of Hyd-2 in electron transport to and from the quinone pool. (A) Strains CP1034 (Δ*hyaB hycE hyfB-R*; black line) and CP1A3 (Δ*hyaB hybA hycE*; gray line) were grown in M9 minimal medium with 0.4% (wt/vol) glycerol and 25 mM fumarate, and the cells were harvested and washed before an amount equivalent to 5 mg protein was added to the chamber of a hydrogen electrode. After a period of equilibration, glycerol was added to a final concentration of 170 mM as indicated. After a further 20 to 30 min of equilibration, fumarate was added to a final concentration of 25 mM as indicated by the arrows. (B) Strains CP1034 (Δ*hyaB hycE hyfB-R*; black line) and CP1A3 (Δ*hyaB hybA hycE*; gray line) were grown in M9 minimal medium with 0.4% (wt/vol) glycerol and 25 mM fumarate, and the cells were harvested and washed before an amount equivalent to 5 mg protein was added to the chamber of a hydrogen electrode. An aliquot of hydrogen-saturated buffer corresponding to 600 nmol was added after 1 min of equilibration. After a further equilibration of the signal of between 5 and 10 min, fumarate was added to a final concentration of 25 mM as indicated by the arrow.

the faster-migrating species of the Hyd-2 activity band (Fig. 4A). This suggests that the faster-migrating band consists of the catalytically active HybOC complex (see also references 7 and 40), while the slower-migrating species consists of different forms of the heteromeric HybOC-AB complex. Reintroduction of plasmid-carried *hybA* into FTD671 restored the more slowly migrating activity band in native PAGE analysis (Fig. 4A).

An experiment comparing the ability of washed, whole cells of IC010 and CP1A3 (Δ*hyaB hybA hycE*) to use reduced methyl viologen dye as an electron donor demonstrated that H_2 production by a Hyd-2 enzyme lacking HybA was similar to that by native Hyd-2 (Fig. 4B). Together, these results indicate that HybA is not required for electron transfer to and from artificial redox-active viologen dyes but that it is necessary for electron flow to and from Hyd-2 via the quinone pool.

The proton gradient drives Hyd-2-dependent H_2 evolution. Having demonstrated that H_2 evolution is dependent on MQ/DMQ, it is important to consider how menaquinol (standard redox potential E'^0 of approximately −80 mV) can drive the endergonic reduction of protons to molecular H_2 (redox potential E'^0 of −418 mV). To examine whether this activity is coupled to the proton gradient, cells of strain IC010 (MC4100 Δ*hyaB hycE*) were incubated with glycerol to induce Hyd-2-dependent H_2 evolution, and then after 10 min of incubation, the uncoupler CCCP was added (Fig. 5A). The results clearly demonstrate that H_2 evolution stopped immediately upon addition of CCCP, which indicates that a proton gradient is required to drive this reaction. After a further 5 min, fumarate was added to the cells and H_2 oxidation commenced (Fig. 5A), indicating that this process was not inhibited by the uncoupler. To confirm that Hyd-2-dependent electron transfer to FRD was independent of the uncoupler CCCP, first, cells of IC010 were incubated with H_2; then, fumarate was added to induce H_2 oxidation; and after 10 min, CCCP was added. The data in Fig. 5B show that CCCP had no effect on fumarate-dependent H_2 oxidation, which is in agreement with the fact that hydrogen oxidation coupled to fumarate reduction (fumarate/succinate

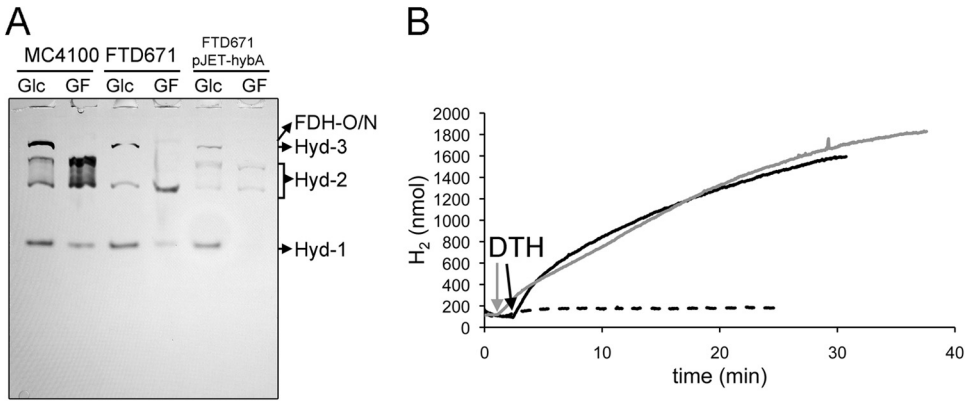

FIG 4 Hyd-2 lacking the HybA subunit retains H_2:viologen dye oxidoreductase activity. (A) Strains MC4100 and FTD671 (Δ*hybA*) and FTD671 complemented with pJET-hybA were grown in GF medium or in glucose medium (Glc), and 25 μg of protein was subjected to native PAGE and subsequently stained for hydrogenase activity as described in Materials and Methods. The migration patterns of Hyd-1 and Hyd-2, as well as the H_2-oxidizing activity of FDH-O and FDH-N, are shown on the right. (B) Strains IC010 (Δ*hyaB hycE*; black line) and CP1A3 (Δ*hyaB hybA hycE*; gray line) were prepared as described for panel A, and an amount of cells corresponding to 5 mg protein was added to the electrode chamber. After a short equilibration, MV was added to the chamber to a final concentration of 1.2 mM and subsequently reduced with sodium dithionite to dark blue (indicated by an arrow and "DTH"). Buffer without cells served as a negative control (dashed line).

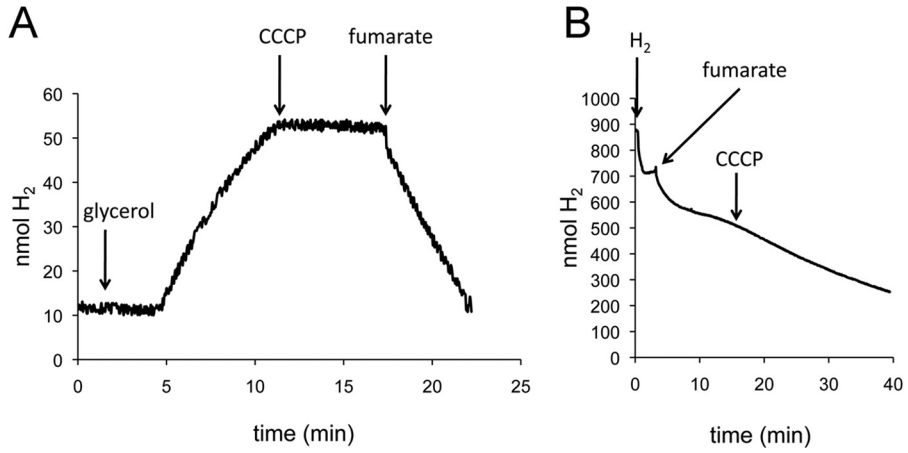

FIG 5 Glycerol-dependent H_2 evolution by Hyd-2 requires a proton gradient. Strain IC010 (Δ*hyaB hycE*) was grown with 25 mM fumarate and 0.4% (vol/vol) glycerol, and cells corresponding to 5 mg of protein were applied to the electrode. (A) After equilibration, glycerol was added to a final concentration of 170 mM as indicated. When H_2 production was linear, CCCP was added to a final concentration of 100 μM as indicated. After about 5 min, fumarate was added to a final concentration of 25 mM as indicated by an arrow. (B) Strain IC010 was added to the electrode, and H_2-saturated buffer was added as indicated. When the signal attained a constant level, fumarate was added to a 25 mM final concentration as indicated. After 10 min of H_2 oxidation, CCCP was added to 100 μM and the signal was recorded for another 20 min.

redox potential E'^0 of +30 mV) is an exergonic reaction and therefore independent of the proton gradient.

An Δ*frdA* strain lacks Hyd-2-linked H_2-dependent benzyl viologen reductase activity during respiration with fumarate. Based on the findings described above, it is possible to switch Hyd-2 between H_2-evolving and H_2-oxidizing modes by altering the growth conditions from glycerol fermentation to glycerol-fumarate respiration, respectively. Moreover, it appears that when electron flow to FRD is interrupted, e.g., by a *menA* mutation (Fig. 2A), the ability of Hyd-2 to reduce BV is somehow impaired, despite the enzyme being immunologically detectable (see Fig. S3 in the supplemental material). In order to investigate the latter phenomenon in more detail, we decided first to generate strain SAL1 (Δ*hyaB* Δ*hycAI* Δ*frdA*), which lacks FRD, and examine the consequences on Hyd-2 activity measured quantitatively in crude extracts (Table 2). We also examined activity in the in-gel Hyd-2 activity assay after growth in glycerol-fumarate medium (Fig. 6A). While the control strain IC010 showed an activity band corresponding to Hyd-2 after growth in GF medium, no activity band could be observed in extracts of SAL1; note that the *hycE* and *hycAI* alleles have identical phenotypes with regard to loss of Hyd-3 activity (41). Hyd-2 activity was reduced approximately 7-fold in extracts of SAL1 compared with extracts of IC010 (Table 2). The total hydrogenase activity in IC010 was similar to that in the wild-type MC4100, while an extract derived from a *hypF* mutant (DHP-F2), which lacks all hydrogenases (42) and acted as a negative control, lacked measurable hydrogenase activity. Determination of FRD enzyme activity in the same extracts revealed that strain SAL1 completely lacked activity while MC4100 (wild type) and IC010 had similar FRD activities (Table 2).

TABLE 2 Analysis of hydrogenase and fumarate reductase activity complementation

Strain and plasmid[a]	Sp act (U mg protein^{-1} ± SD[b])	
	Hydrogenase	Fumarate reductase
MC4100	0.19 ± 0.03	0.20 ± 0.03
DHP-F2 (Δ*hypF*)	<0.01	ND[c]
CP1037 (Δ*hyaB* Δ*hycAI*)	0.15 ± 0.05	ND
IC010 (Δ*hyaB hycE*)	0.15 ± 0.06	0.20 ± 0.10
SAL1 (Δ*hyaB* Δ*hycAI* Δ*frdA*)	0.02 ± 0.01	<0.01
SAL1/pACYCDuet-frdAD	0.11 ± 0.02	0.42 ± 0.04
JW4115 (Δ*frdA*)	0.23 ± 0.16	<0.01
JW4115 (Δ*frdA*)/pACYCDuet-frdAD	0.25 ± 0.02	0.40 ± 0.20

[a] Strains were grown for 16 h in M9 minimal medium containing 0.4% glycerol and 25 mM fumarate.
[b] Means and standard deviations of at least three independent measurements are shown.
[c] ND, not determined.

To ensure that the effects of the *frdA* mutation were exclusively due to the deletion of the *frdA* gene, strain SAL1 was complemented with a plasmid carrying the *frdA* gene and Hyd-2 enzyme activity was restored after growth of the strain in GF medium, as was observed in the in-gel assay (Fig. 6A) and by quantitative measurement of enzyme activity (Table 2). The reappearance of Hyd-2 activity under GF growth conditions correlated with the recovery of FRD activity in the complemented SAL1 strain (Table 2). Together, these results indicate that by preventing electron flow to FRD, even in the presence of fumarate, no H_2:BV oxidoreductase activity of Hyd-2 could be detected in crude extracts separated in nondenaturing gels. Activity could be restored, however, by reintroducing the *frdABCD* operon on a plasmid.

The *E. coli* Hyd enzymes are active across a wide range of redox potentials and in the presence of different electron acceptors (23, 32). As well as fumarate, electron transport chains coupling H_2 oxidation to dimethyl sulfoxide (DMSO) and TMAO have also been described (14). Even in the absence of externally added electron acceptors, glycerol can function as a sole carbon source in minimal medium as long as the culture is supplemented with Casamino Acids to permit growth (20). An extract derived from the wild-type MC4100 grown anaerobically in glycerol and Casamino Acids medium lacked Hyd-2 enzyme activity after native PAGE (Fig. 6B, lane 4). Activity of Hyd-1, while reduced compared to that in extracts of MC4100 cells grown with glucose, was clearly visible. Growth in the presence of either fumarate, TMAO,

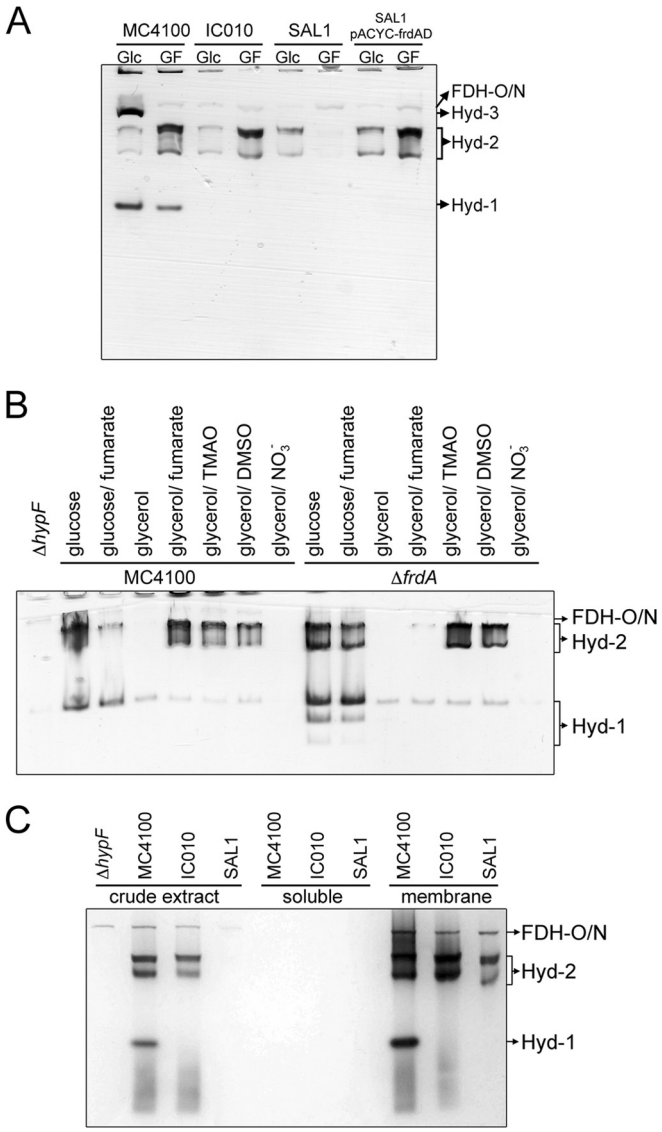

FIG 6 Δ*frdA* strain lacks hydrogen: BV-oxidoreductase activity of hydrogenase 2. (A) Strains MC4100, IC010 (Δ*hyaB hycE*), and SAL1 (Δ*hyaB hycAI frdA*) and SAL1 complemented with pACYC-frdAD were grown anaerobically in M9 minimal medium containing either 0.8% (wt/vol) glucose (Glc) or 0.4% (vol/vol) glycerol and 25 mM fumarate (GF). Extracts with 25 μg of protein were subjected to native PAGE, and subsequently, the gel was stained for hydrogenase activity as described in Materials and Methods. The migration patterns of the hydrogenase-independent formate dehydrogenases O and N (FDH-O/N) as well as Hyd-1 through Hyd-3 are labeled. (B) Cells of MC4100, DHP-F2 (Δ*hypF*), and JW4115 (Δ*frdA*) were grown in M9 minimal medium as described in Materials and Methods with 0.8% (wt/vol) glucose or 0.8% (vol/vol) glycerol as the carbon source. The electron acceptor sodium fumarate, sodium nitrate (NO_3^-), TMAO, or DMSO was added where indicated to a final concentration of 25 mM. Equivalent amounts of protein (25 μg) were loaded on native PAGE gels, and after electrophoresis, the gel was stained for hydrogenase activity. The bands are labeled as FDH-O/N for hydrogenase-independent formate dehydrogenase O and N activities and Hyd-2 and Hyd-1 for hydrogenases 2 and 1, respectively. (C) Strains DHP-F2 (Δ*hypF*), MC4100, IC010, and SAL1 were grown in 0.4% (vol/vol) glycerol and 25 mM fumarate (GF), and the crude extracts as well as cytosolic fraction (soluble) and membrane fraction (membrane) were prepared as described in reference 11. Aliquots of the subcellular fractions (25 μg of protein) were loaded on a native PAGE gel and subsequently subjected to hydrogenase activity staining. The migration patterns of FDH-O/N, Hyd-1, and Hyd-2 are labeled.

or DMSO revealed that active Hyd-2 and Hyd-1 enzymes were detectable (Fig. 6B) (12). In the presence of nitrate, a different respiratory chain involving a nitrate-dependent formate dehydrogenase (FDH-N) and nitrate reductase is employed and no Hyd activity is detectable (43). This is due to NarL, the nitrate response regulator, preventing the transcription of genes encoding both respiratory hydrogenases (44). The results of these experiments indicate that during glycerol fermentation in M9 minimal medium the dye-reducing activity of Hyd-2 is undetectable in stationary-phase cultures, which correlates with Hyd-2 acting in proton reduction mode.

In order to address the question whether the effects of introducing the Δ*frdA* allele into strain BW25113 (Table 1) would cause the same Hyd-2 activity phenotype, we analyzed extracts of strain JW4115 after growth under the same fermentative and respiratory conditions used to test Hyd-2 activity in MC4100 (Fig. 6B). Clearly, neither fermentative growth with glucose nor respiration with DMSO or TMAO affected either Hyd-1 or Hyd-2 enzyme activities. However, after growth in glycerol and Casamino Acids, no Hyd-2 activity could be detected, while after growth in GF medium, only a very weak Hyd-2 activity band was observed; in contrast, Hyd-1 enzyme activity was unaffected under these conditions. Western blot analysis of cell extract derived from the *frdA* mutant revealed nearly wild-type levels of HybC, the catalytic subunit of Hyd-2, after growth in GF medium (see Fig. S3 in the supplemental material). Thus, the phenotype of an *frdA* strain grown in GF medium with regard to Hyd-2 activity is comparable with that of the wild type after growth under glycerol fermentation. Note that FRD activity was abolished in an extract of strain JW4115 (Δ*frdA*) but was recovered by reintroducing the *frdA* gene on a plasmid (Table 2). Because strain JW4115 has the capacity to synthesize all four hydrogenases, the total hydrogenase enzyme activity of the strain was hardly affected by the *frdA* mutation because lack of Hyd-2 activity was complemented presumably by a corresponding increase in the activities of Hyd-1, Hyd-3, and/or Hyd-4 (45).

Hyd-2 activity can be recovered in the membrane fraction of *frdA* mutants. In order to examine further the biochemical cause of the lack of Hyd-2 dye-reducing enzyme activity in *frdA* mutants, cells of isogenic strains MC4100, IC010 (Δ*hyaB* Δ*hycE*), and SAL1 (Δ*hyaB* Δ*hycAI* Δ*frdA*) were grown anaerobically in GF medium, the crude extract was subsequently separated into soluble and membrane fractions by ultracentrifugation, and these subcellular fractions were assayed for hydrogen-oxidizing activity with benzyl viologen after native PAGE (Fig. 6C). While no Hyd-2 activity in a crude extract of strain SAL1 was detectable, Hyd-2 enzyme activity was recovered in the membrane fraction after subcellular fractionation of the crude extract. H_2:BV oxidoreductase activities of Hyd-1 in strain MC4100 and of FDH-N/O (46) in all three strains acted as controls, demonstrating that all three activities were exclusively detected in the membrane fraction. This result indicates that the apparent inhibition of H_2:BV oxidoreductase activity observed in crude extracts in the *frdA* mutant was reversible.

Quantitative analysis of H_2 production by Hyd-2. Due to the fact that FRD is menaquinone dependent (47), our findings suggest that Hyd-2 can no longer oxidize hydrogen if electron transfer through the menaquinone pool is impeded. Thus, an impediment in menaquinone biosynthesis and also deletion of the genes encoding FRD or growth on glycerol without provision of an exter-

TABLE 3 Hydrogen production during glucose, glycerol, and glycerol/fumarate growth[a]

Strain	Hydrogen produced after growth with:		
	0.4% glycerol	0.4% glycerol-25 mM fumarate	0.8% glucose
MC4100	3.15 ± 0.87	0.67 ± 0.09	1.93 ± 0.52
CP887 (Δ*frdA*)	2.99 ± 0.95	2.27 ± 0.30	1.56 ± 0.25
HDK200 (Δ*hybBC*)	1.64 ± 0.43	0.66 ± 0.35	2.36 ± 0.58
SAL1 (Δ*hyaB hycAI frdA*)	1.84 ± 0.33	2.17 ± 0.91	0.04 ± 0
FTD147 (Δ*hyaB hybC hycE*)	<0.01	<0.01	<0.01

[a] Samples were drawn from the headspace after 26 h of growth and calculated according to the optical density as U ml^{-1} unit of optical density at 600 nm^{-1}.

nal electron acceptor both cause a similar phenotype in which dye-reducing activity of Hyd-2 is inhibited in crude extracts.

If electrons cannot be delivered to FRD during growth on glycerol, then it is likely that the electrons will be used to reduce protons and generate hydrogen via Hyd-2 (e.g., Fig. 2). It has been observed that no H_2 accumulates during growth in GF medium, where a respiratory electron acceptor is plentiful (7), despite the findings of recent studies (22) clearly showing that during glycerol fermentation Hyd-2 can contribute to H_2 production. Moreover, *in vitro* studies using purified Hyd-2 have shown that the enzyme can catalyze hydrogen production at low redox potentials (23). Therefore, we analyzed H_2 production in the culture headspace after growth of various mutants in GF medium. Our experiments showed that during growth of MC4100 in GF medium, only a small amount H_2 is present in the headspace (Table 3). No hydrogen was detectable in a strain where the main uptake and evolving Hyd enzymes are missing (FTD147, Δ*hyaB hybC hycE*). In the *frdA* deletion strain (CP887), more than 3 times as much H_2 was produced as in its parental strain MC4100. A strain deficient in Hyd-2 synthesis (HDK200) showed a level of H_2 accumulation (0.66 units) similar to that observed for MC4100, indicating that Hyd-2 was not the only enzyme responsible for H_2 production under these conditions. Strain SAL1 (Δ*hyaB* Δ*hycAI* Δ*frdA*) exhibited high levels of H_2 evolution, similar to those produced by the Δ*frdA* mutant CP887 (Table 3).

The data in Table 3 show that when MC4100 was grown with glycerol but without fumarate, this also yielded high levels of H_2 production (3.15 units). In contrast, strains HDK200 (Δ*hybBC*) and SAL1 (Δ*hyaB hycAI frdA*) both had approximately 50% of this level of H_2 production. Together, these results indicate that under conditions where no H_2 oxidation by Hyd-2 is detectable (Table 2 and Fig. 6), at least 50% of the H_2 generated under these conditions derives from Hyd-2. Furthermore, these findings indicate that Hyd-2 switches between hydrogen-consuming and hydrogen-producing roles *in vivo*.

DISCUSSION

In this study, we have investigated the physiology and bioenergetics of bidirectional H_2 activation by Hyd-2 during anaerobic metabolism of glycerol. Our findings reveal that MQ/DMQ is required for electron transfer to and from Hyd-2 under these conditions, that the HybA subunit is essential to mediate electron transfer between the enzyme and the quinone pool, and, significantly, that the proton gradient drives H_2 evolution catalyzed by Hyd-2. These features of Hyd-2 are summarized in the working model presented in Fig. 7.

Under respiratory conditions where excess electron acceptor is available, Hyd-2 functions as an H_2-oxidizing enzyme. During glucose fermentation at high substrate concentration, H_2 accumulates only in strains that are able to form an intact FHL complex but not in strains where *hyc* genes are deleted (2). This result shows that strains unable to synthesize FRD are not impaired in glucose fermentation, which agrees with previous observations (48). Under conditions of fumarate-dependent respiration of glycerol, Hyd-2 is synthesized, active, and poised to oxidize H_2, passing the derived electrons to the quinone pool. This H_2 oxidation activity of Hyd-2 is readily assayed using redox dyes either in solution or after separation of the enzyme complexes by native PAGE (11). The enzyme is able to recycle hydrogen generated, for example, by the FHL complex, coupling H_2 oxidation to fumarate reduction (Fig. 7). Glycerol is converted to dihydroxyacetone-3-phosphate (DHAP) by the combined actions of glycerol kinase and glycerol-3-phosphate dehydrogenase (GlpK/G-3P DH) (17). The reducing equivalents derived from glycerol enter the quinone pool and are reoxidized by reducing fumarate to succinate catalyzed by FRD (33, 39).

On the other hand, if cells are supplied with only glycerol or if FRD is genetically inactivated, Hyd-2 is still synthesized but catalyzes H_2 evolution, which presumably prevents overreduction of the quinone pool during glycerol fermentation (Fig. 7). Anaerobic glycerol oxidation can occur either via GlpK/G-3P DH or via glycerol dehydrogenase (GldA), which generates NADH (19). Coupling of glycerol-3 phosphate oxidation to proton reduction via MQH_2 is possible, as depicted in Fig. 7, and this could be linked to H_2 evolution by Hyd-2. However, recent studies (19) have suggested that GldA and dihydroxyacetone kinase (DHAK) also have key roles in glycerol fermentation. Theoretically, NADH oxidation can be accomplished by exclusive conversion of acetyl coenzyme A (acetyl-CoA) to ethanol via alcohol dehydrogenase; however, in wild-type *E. coli* this would obviate the production of H_2 by Hyd-2, and instead, H_2 would be produced from formate via FHL, as we have also observed in this study. Nevertheless, a mutant synthesizing only Hyd-2 was also capable of producing H_2 from glycerol, suggesting that if the GlpK/G-3P DH route is used, G-3P DH couples electron transfer to Hyd-2 via MQ, or alternatively, in the absence of a functional FHL in the mutant, the GldA route operates and formate is excreted into the periplasm where it could be oxidized by FDH-O (46) with concomitant electron transfer to Hyd-2 via MQ. A further alternative would involve generating a mixture of acetate and ethanol; however, complete redox balance could then be achieved only if reoxidation of the NADH generated by GldA could be coupled to H_2 evolution by Hyd-2 through an MQ-coupled NADH oxidase activity, which has been observed previously (49).

All of these possible routes of linking the excess redox equivalents generated by glycerol fermentation to H_2 evolution are complicated by the novel finding of this study that proton reduction catalyzed by Hyd-2 is dependent on the proton motive force (PMF). Each of the three possible energy sources, i.e., formate, G-3P, or NADH, at physiological concentrations could theoretically allow H_2 production by Hyd-2, but this does not readily explain why the PMF is linked to H_2 evolution. Hyd-2 has an unusual structure for a modular membrane-associated oxidoreductase in that, as well as having a typical electron-transferring small subunit, HybO, it also has the additional electron-

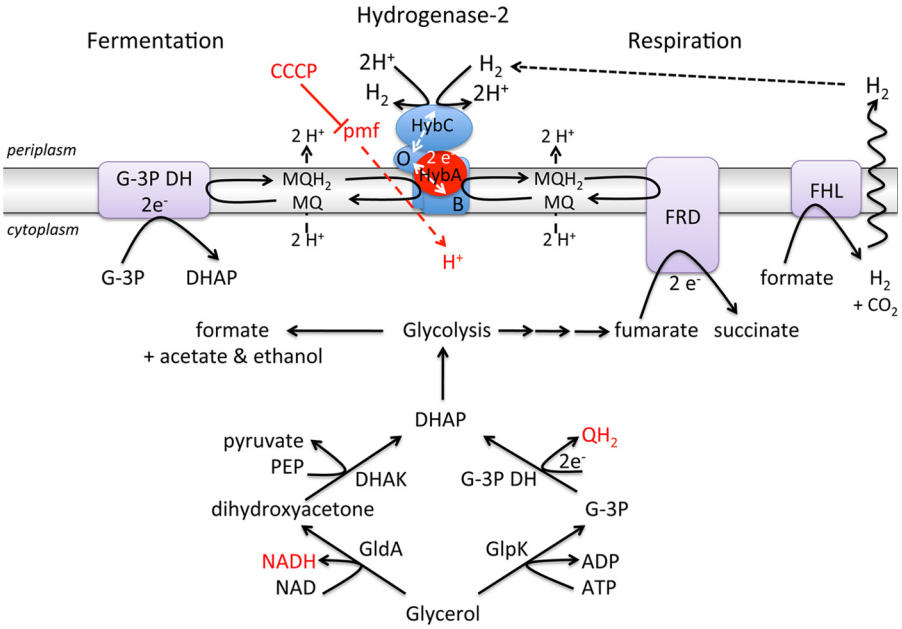

FIG 7 Model depicting the function of Hyd-2 during glycerol fermentation and glycerol-fumarate respiration. A schematic representation of the anaerobic metabolism of glycerol is shown in the lower portion of the figure. The reduced products of anaerobic glycerol metabolism are shown in red letters. Note that the enzymes glycerol dehydrogenase (GldA), glycerol kinase (GlpK), and glycerol-3 phosphate dehydrogenase (G-3P DH) are normally membrane-associated enzymes. The upper portion of the figure depicts how Hyd-2 is involved in glycerol fermentation (left side) or glycerol respiration (right side). The red dashed line indicates that a proton motive force (PMF) drives the electron transfer from glycerol via menaquinol to Hyd-2. The solid red line indicates that CCCP blocks H_2 production by Hyd-2. The dashed black line signifies that hydrogen generated by the formate hydrogenlyase (FHL) complex can be reoxidized by Hyd-2. The Hyd-2 enzyme comprises the HybOABC subunits, and HybA, which is required for electron transfer to and from the quinone pool (see the text), is highlighted in red. Electron transfer within the Hyd-2 complex is represented by dashed white lines. The other protein complex represented in purple is fumarate reductase (FRD). Abbreviations: DHAK, dihydroxyacetone kinase; DHAP, dihydroxyacetone phosphate; QH_2, reduced quinone; MQ/MQH_2, menaquinone/menaquinol; PEP, phosphoenolpyruvate.

transferring HybA subunit. HybA has been shown here to be essential for H_2 evolution catalyzed by the enzyme. Furthermore, the membrane anchor subunit HybB is atypical in modular oxidoreductases because it lacks cofactors (7). It is conceivable therefore that HybB operates as a conformational proton pump when electrons are channeled through the enzyme to the quinone pool. This would imply that when Hyd-2 operates in the H_2-evolving mode, it requires a PMF, while in the opposite H_2-oxidizing mode, it helps generate a proton gradient. This would also explain why the enzyme is inhibited by an uncoupler when it is working in the H_2 evolution direction but not when it functions in the H_2-oxidizing direction. Indeed, there is an indication that the uncoupler slightly speeds up fumarate reduction (Fig. 5), which would support this hypothesis.

We have shown here that the HybA subunit of Hyd-2 is required to mediate bidirectional electron transfer with MQ and that it is necessary to facilitate reverse electron transport to allow H_2 evolution. Surprisingly, we observed a correlation between the enzyme working as a proton reductase and a concomitant inability to detect the enzyme's H_2-oxidizing activity when assayed with redox dyes *in vitro*. This suggests that, under certain circumstances, electron flow through Hyd-2 might somehow be modified to maintain a bias toward one reaction direction. It is currently unclear what the underlying mechanistic basis of this catalytic bias might be. Remarkably, however, it was possible to restore dye-reducing activity to Hyd-2 *in vitro* by separating the membrane and cytoplasmic fractions. One possible explanation for this finding is that H_2-dependent dye-reducing activity is reversibly inhibited by overreduction of the iron-sulfur clusters in the HybO and HybA subunits of the enzyme, although treatment of crude extracts with oxidants such as ferricyanide or performing the electrophoresis under aerobic conditions failed to restore this activity to Hyd-2 in crude extracts (data not shown). An alternative explanation is that Hyd-2 enzyme activity is inhibited by a component in the soluble subcellular fraction; however, remixing of the soluble and membrane fractions after their physical separation failed to restore inhibition of Hyd-2 enzyme activity. Clearly, further experiments will be required to elucidate the biochemical mechanism underlying the reversible inhibition of redox dye-reducing activity.

In summary, our findings indicate that Hyd-2 is clearly able to switch between H_2 oxidation and H_2 production modes without altering protein content and without expending energy on *de novo* protein synthesis. This is important to allow metabolic flexibility of H_2 metabolism, and it also possibly explains why *E. coli* has evolved two routes of anaerobic glycerol utilization (19). The two routes likely operate simultaneously to provide a balanced redox status of the quinone pool and an optimal proton gradient (Fig. 7). H_2 production by Hyd-2 observed in this study places in a new context the recent finding that deletion of genes encoding Hyd-2 has a deleterious effect on H_2 production during glycerol fermentation (17) and provides an explanation for the suggested Hyd-2-dependent H_2 evolution during glycerol fermentation in another recent study (50). Moreover, our study provides the first demonstration that H_2 evolution by Hyd-2 is directly linked to the PMF.

ACKNOWLEDGMENTS

This work was supported by the BBSRC grants BB/I02008X/1 and BB/L008521/1 to F.S. and by the Deutsche Forschungsgemeinschaft (no. SA 494/3-2) to R.G.S.

S.L. carried out experiments whose results are shown in Fig. 6 and Table 2. S.L. and C.P. carried out the strain constructions for this study. M.J. and C.L.K. carried out the H_2 headspace measurements. C.L.K. performed the H_2 electrode experiments leading to Fig. 1. C.P. carried out all other experiments. C.P., F.S., and R.G.S. drafted the manuscript and conceived the study. All authors read and approved the final manuscript.

We declare that we have no competing interest.

REFERENCES

1. **Krebs HA.** 1937. The role of fumarate in the respiration of *Bacterium coli commune*. Biochem J **31:**2095–2124.
2. **Forzi L, Sawers RG.** 2007. Maturation of [NiFe]-hydrogenases in *Escherichia coli*. Biometals **20:**565–578. http://dx.doi.org/10.1007/s10534-006-9048-5.
3. **Böck A, King P, Blokesch M, Posewitz M.** 2006. Maturation of hydrogenases. Adv Microb Physiol **51:**1–71. http://dx.doi.org/10.1016/S0065-2911(06)51001-X.
4. **Sargent F, Stanley NR, Berks BC, Palmer T.** 1999. Sec-independent protein translocation in *Escherichia coli*. A distinct and pivotal role for the TatB protein. J Biol Chem **274:**36073–36082. http://dx.doi.org/10.1074/jbc.274.51.36073.
5. **Brøndsted L, Atlung T.** 1994. Anaerobic regulation of the hydrogenase 1 (*hya*) operon of *Escherichia coli*. J Bacteriol **176:**5423–5428.
6. **Lukey MJ, Roessler MM, Parkin A, Evans RM, Davies RA, Lenz O, Friedrich B, Sargent F, Armstrong FA.** 2011. Oxygen-tolerant [NiFe]-hydrogenases: the individual and collective importance of supernumerary cysteines at the proximal Fe-S cluster. J Am Chem Soc **133:**16881–16892. http://dx.doi.org/10.1021/ja205393w.
7. **Dubini A, Pye R, Jack R, Palmer T, Sargent F.** 2002. How bacteria get energy from hydrogen: a genetic analysis of periplasmic hydrogen oxidation in *Escherichia coli*. Int J Hydrogen Energy **27:**1413–1420. http://dx.doi.org/10.1016/S0360-3199(02)00112-X.
8. **Sargent F, Ballantine S, Rugman P, Palmer T, Boxer D.** 1998. Reassignment of the gene encoding the *Escherichia coli* hydrogenase 2 small subunit-identification of a soluble precursor of the small subunit in a *hypB* mutant. Eur J Biochem **255:**746–754. http://dx.doi.org/10.1046/j.1432-1327.1998.2550746.x.
9. **McDowall JS, Murphy BJ, Haumann M, Palmer T, Armstrong FA, Sargent F.** 2014. Bacterial formate hydrogenlyase complex. Proc Natl Acad Sci U S A **111:**E3948–E3956. http://dx.doi.org/10.1073/pnas.1407927111.
10. **Pinske C, Sawers RG.** 2014. The importance of iron in the biosynthesis and assembly of [NiFe]-hydrogenases. Biomol Concepts **5:**55–70. http://dx.doi.org/10.1515/bmc-2014-0001.
11. **Ballantine S, Boxer D.** 1985. Nickel-containing hydrogenase isoenzymes from anaerobically grown *Escherichia coli* K-12. J Bacteriol **163:**454–459.
12. **Sawers RG, Ballantine S, Boxer D.** 1985. Differential expression of hydrogenase isoenzymes in *Escherichia coli* K-12: evidence for a third isoenzyme. J Bacteriol **164:**1324–1331.
13. **Sawers RG.** 1985. Membrane-bound hydrogenase isoenzymes of *Escherichia coli*. Ph.D. thesis. Department of Biochemistry, University of Dundee, Dundee, Scotland.
14. **Unden G, Bongaerts J.** 1997. Alternative respiratory pathways of *Escherichia coli*: energetics and transcriptional regulation in response to electron acceptors. Biochim Biophys Acta **1320:**217–234. http://dx.doi.org/10.1016/S0005-2728(97)00034-0.
15. **Macy J, Kulla H, Gottschalk G.** 1976. H2-dependent anaerobic growth of *Escherichia coli* on L-malate: succinate formation. J Bacteriol **125:**423–428.
16. **Iverson TM, Luna-Chavez C, Cecchini G, Rees DC.** 1999. Structure of the *Escherichia coli* fumarate reductase respiratory complex. Science **284:**1961–1966. http://dx.doi.org/10.1126/science.284.5422.1961.
17. **Tran KT, Maeda T, Wood TK.** 2014. Metabolic engineering of *Escherichia coli* to enhance hydrogen production from glycerol. Appl Microbiol Biotechnol **98:**4757–4770. http://dx.doi.org/10.1007/s00253-014-5600-3.
18. **Dharmadi Y, Murarka A, Gonzalez R.** 2006. Anaerobic fermentation of glycerol by *Escherichia coli*: a new platform for metabolic engineering. Biotechnol Bioeng **94:**821–829. http://dx.doi.org/10.1002/bit.21025.
19. **Cintolesi A, Clomburg JM, Rigou V, Zygourakis K, Gonzalez R.** 2012. Quantitative analysis of the fermentative metabolism of glycerol in *Escherichia coli*. Biotechnol Bioeng **109:**187–198. http://dx.doi.org/10.1002/bit.23309.
20. **Gonzalez R, Murarka A, Dharmadi Y, Yazdani SS.** 2008. A new model for the anaerobic fermentation of glycerol in enteric bacteria: trunk and auxiliary pathways in *Escherichia coli*. Metab Eng **10:**234–245. http://dx.doi.org/10.1016/j.ymben.2008.05.001.
21. **Murarka A, Dharmadi Y, Yazdani SS, Gonzalez R.** 2008. Fermentative utilization of glycerol by *Escherichia coli* and its implications for the production of fuels and chemicals. Appl Environ Microbiol **74:**1124–1135. http://dx.doi.org/10.1128/AEM.02192-07.
22. **Trchounian K, Soboh B, Sawers RG, Trchounian A.** 2013. Contribution of hydrogenase 2 to stationary phase H2 production by *Escherichia coli* during fermentation of glycerol. Cell Biochem Biophys **66:**103–108. http://dx.doi.org/10.1007/s12013-012-9458-7.
23. **Lukey MJ, Parkin A, Roessler MM, Murphy BJ, Harmer J, Palmer T, Sargent F, Armstrong FA.** 2010. How *Escherichia coli* is equipped to oxidize hydrogen under different redox conditions. J Biol Chem **285:**3928–3938. http://dx.doi.org/10.1074/jbc.M109.067751.
24. **Miller JH.** 1972. Experiments in molecular genetics. Cold Spring Harbor Laboratory Press, Cold Spring Harbor, NY.
25. **Hormann K, Andreesen J.** 1989. Reductive cleavage of sarcosine and betaine by *Eubacterium acidaminophilum* via enzyme systems different from glycine reductase. Arch Microbiol **153:**50–59. http://dx.doi.org/10.1007/BF00277541.
26. **Sambrook J, Russell D.** 2001. Molecular cloning: a laboratory manual, 3rd ed. Cold Spring Harbor Laboratory Press, Cold Spring Harbor, NY.
27. **Baba T, Ara T, Hasegawa M, Takai Y, Okumura Y, Baba M, Datsenko K, Tomita M, Wanner B, Mori H.** 2006. Construction of *Escherichia coli* K-12 in-frame, single-gene knockout mutants: the Keio collection. Mol Syst Biol **2:**2006. 0008. http://dx.doi.org/10.1038/msb4100050.
28. **Skibinski DAG, Golby P, Chang Y-S, Sargent F, Hoffman R, Harper R, Guest JR, Attwood MM, Berks BC, Andrews SC.** 2002. Regulation of the hydrogenase-4 operon of *Escherichia coli* by the sigma(54)-dependent transcriptional activators FhlA and HyfR. J Bacteriol **184:**6642–6653. http://dx.doi.org/10.1128/JB.184.23.6642-6653.2002.
29. **Laemmli U.** 1970. Cleavage of structural proteins during the assembly of the head of bacteriophage T4. Nature **227:**680–685. http://dx.doi.org/10.1038/227680a0.
30. **Towbin H, Staehelin T, Gordon J.** 1979. Electrophoretic transfer of proteins from polyacrylamide gels to nitrocellulose sheets: procedure and some applications. Proc Natl Acad Sci U S A **76:**4350–4354. http://dx.doi.org/10.1073/pnas.76.9.4350.
31. **Magalon A, Böck A.** 2000. Dissection of the maturation reactions of the [NiFe] hydrogenase 3 from *Escherichia coli* taking place after nickel incorporation. FEBS Lett **473:**254–258. http://dx.doi.org/10.1016/S0014-5793(00)01542-8.
32. **Pinske C, Jaroschinsky M, Sargent F, Sawers RG.** 2012. Zymographic differentiation of [NiFe]-hydrogenases 1, 2 and 3 of *Escherichia coli* K-12. BMC Microbiol **12:**134. http://dx.doi.org/10.1186/1471-2180-12-134.
33. **Spencer ME, Guest JR.** 1973. Isolation and properties of fumarate reductase mutants of *Escherichia coli*. J Bacteriol **114:**563–570.
34. **Bradford MM.** 1976. A rapid and sensitive method for the quantitation of microgram quantities of protein utilizing the principle of protein-dye binding. Anal Biochem **72:**248–254. http://dx.doi.org/10.1016/0003-2697(76)90527-3.
35. **Jones RW.** 1980. The role of the membrane-bound hydrogenase in the energy-conserving oxidation of molecular hydrogen by *Escherichia coli*. Biochem J **188:**345–350.
36. **Ballantine S, Boxer D.** 1986. Isolation and characterisation of a soluble active fragment of hydrogenase isoenzyme 2 from the membranes of anaerobically grown *Escherichia coli*. Eur J Biochem **156:**277–284. http://dx.doi.org/10.1111/j.1432-1033.1986.tb09578.x.
37. **Suvarna K, Stevenson D, Meganathan R, Hudspeth ME.** 1998. Menaquinone (vitamin K2) biosynthesis: localization and characterization of the *menA* gene from *Escherichia coli*. J Bacteriol **180:**2782–2787.
38. **Pinske C, Sawers RG.** 2012. Delivery of iron-sulfur clusters to the hydrogen-oxidizing [NiFe]-hydrogenases in *Escherichia coli* requires the A-type carrier proteins ErpA and IscA. PLoS One **7:**e31755. http://dx.doi.org/10.1371/journal.pone.0031755.
39. **Wissenbach U, Ternes D, Unden G.** 1992. An *Escherichia coli* mutant containing only demethylmenaquinone, but no menaquinone: effects on fu-

marate, dimethylsulfoxide, trimethylamine *N*-oxide and nitrate respiration. Arch Microbiol **158:**68–73. http://dx.doi.org/10.1007/BF00249068.

40. **Jack RL, Buchanan G, Dubini A, Hatzixanthis K, Palmer T, Sargent F.** 2004. Coordinating assembly and export of complex bacterial proteins. EMBO J **23:**3962–3972. http://dx.doi.org/10.1038/sj.emboj.7600409.
41. **Pinske C, Krüger S, Soboh B, Ihling C, Kuhns M, Braussemann M, Jaroschinsky M, Sauer C, Sargent F, Sinz A, Sawers RG.** 2011. Efficient electron transfer from hydrogen to benzyl viologen by the [NiFe]-hydrogenases of *Escherichia coli* is dependent on the coexpression of the iron-sulfur cluster-containing small subunit. Arch Microbiol **193:**893–903. http://dx.doi.org/10.1007/s00203-011-0726-5.
42. **Paschos A, Bauer A, Zimmermann A, Zehelein E, Böck A.** 2002. HypF, a carbamoyl phosphate-converting enzyme involved in [NiFe] hydrogenase maturation. J Biol Chem **277:**49945–49951. http://dx.doi.org/10.1074/jbc.M204601200.
43. **Wimpenny JW, Cole JA.** 1967. The regulation of metabolism in facultative bacteria. The effect of nitrate. Biochim Biophys Acta **148:**233–242. http://dx.doi.org/10.1016/0304-4165(67)90298-X.
44. **Richard D, Sawers RG, Sargent F, McWalter L, Boxer D.** 1999. Transcriptional regulation in response to oxygen and nitrate of the operons encoding the [NiFe] hydrogenases 1 and 2 of *Escherichia coli*. Microbiology **145:**2903–2912.
45. **Trchounian A, Sawers RG.** 2014. Novel insights into the bioenergetics of mixed-acid fermentation: can hydrogen and proton cycles combine to help maintain a proton motive force? IUBMB Life **66:**1–7. http://dx.doi.org/10.1002/iub.1236.
46. **Soboh B, Pinske C, Kuhns M, Waclawek M, Ihling C, Trchounian K, Trchounian A, Sinz A, Sawers RG.** 2011. The respiratory molybdoselenoprotein formate dehydrogenases of *Escherichia coli* have hydrogen: benzyl viologen oxidoreductase activity. BMC Microbiol **11:**173. http://dx.doi.org/10.1186/1471-2180-11-173.
47. **Lambden PR, Guest JR.** 1976. Mutants of *Escherichia coli* K12 unable to use fumarate as an anaerobic electron acceptor. J Gen Microbiol **97:**145–160. http://dx.doi.org/10.1099/00221287-97-2-145.
48. **Hu H, Wood TK.** 2010. An evolved *Escherichia coli* strain for producing hydrogen and ethanol from glycerol. Biochem Biophys Res Commun **391:**1033–1038. http://dx.doi.org/10.1016/j.bbrc.2009.12.013.
49. **Singh AP, Bragg PD.** 1975. Reduced nicotinamide adenine dinucleotide dependent reduction of fumarate coupled to membrane energization in a cytochrome deficient mutant of *Escherichia coli* K12. Biochim Biophys Acta **396:**229–241. http://dx.doi.org/10.1016/0005-2728(75)90037-7.
50. **Trchounian K, Sanchez-Torres V, Wood TK, Trchounian A.** 2011. *Escherichia coli* hydrogenase activity and H2 production under glycerol fermentation at a low pH. Int J Hydrogen Energy **36:**4323–4331. http://dx.doi.org/10.1016/j.ijhydene.2010.12.128.
51. **Casadaban MJ.** 1976. Transposition and fusion of the *lac* genes to selected promoters in *Escherichia coli* using bacteriophage lambda and Mu. J Mol Biol **104:**541–555. http://dx.doi.org/10.1016/0022-2836(76)90119-4.
52. **Deplanche K, Caldelari I, Mikheenko IP, Sargent F, Macaskie LE.** 2010. Involvement of hydrogenases in the formation of highly catalytic Pd(0) nanoparticles by bioreduction of Pd(II) using *Escherichia coli* mutant strains. Microbiology **156:**2630–2640. http://dx.doi.org/10.1099/mic.0.036681-0.
53. **Blokesch M, Magalon A, Böck A.** 2001. Interplay between the specific chaperone-like proteins HybG and HypC in maturation of hydrogenases 1, 2, and 3 from *Escherichia coli*. J Bacteriol **183:**2817–2822. http://dx.doi.org/10.1128/JB.183.9.2817-2822.2001.